

Damage Detection as Inverse Problems for Distributed Parameter Systems: Computational Approaches

H.T. Banks

Center for Research in Scientific Computation
North Carolina State University
Raleigh, NC 27695-8205

R.C. Smith

Department of Mathematics
Iowa State University
Ames, IA 50011

Yue Zhang

Center for Research in Scientific Computation
North Carolina State University
Raleigh, NC 27695-8205

Abstract

In this review paper, we outline a theoretical and computational methodology that has been used with success in several nondestructive damage detection and characterization problems. Brief discussions on application to two examples (thermal tomography and vibration testing in structures) are given. A comparison between a spline-based Galerkin method and standard finite element approaches in the context of these problems is presented.

1 Introduction

In this brief review, we discuss an approach to nondestructive evaluation (NDE) techniques that has proven theoretically, computationally and experimentally successful in a wide range of applications. The basic tenet involves treating damage detection and characterization as inverse problems for distributed parameter systems (DPS) with spatially varying coefficients and parameters. In this context one seeks to detect changes in the system due to damage by detecting changes in fundamental physical parameters (thermal conductivity or diffusivity, structural mass density, stiffness, damping, etc.) that appear as coefficients in models describing the system. The approach therefore entails, in an essential way, the development of physical models for the systems being investigated for damages or system changes.

We illustrate these ideas with two examples, presented in more detail elsewhere, with which we have demonstrated the efficacy of our approach. The first example discussed below involves thermal-based NDE methods ([4, 5, 6]). In this case, one has a body with damage

(represented by an unknown boundary that is not directly observable) which one seeks to identify by using thermal probes and infrared sensors on a known observable surface of the body. These problems, which might be considered in the framework of “domain identification” or “shape optimization” problems, can be converted to problems containing DPS with unknown coefficients using a technique known as the “method of mappings” that has been widely used in the area of shape design.

A second class of examples involve the use of routine vibration testing of structures to detect changes in physical characteristics (e.g., stiffness, damping) due to damage induced changes in the structure. While the underlying ideas have been controversial in the engineering literature when used in conjunction with modal methods and frequency shift approaches, we have shown ([2, 11]) they can be used quite effectively in the context of identification of spatially varying coefficients in DPS. We shall briefly outline the approach below using a simple beam with damage due to a small circular hole.

In each of these examples our approach consists of writing a dynamic model involving unknown coefficients and/or boundary terms in a weak or variational form. We then formulate an infinite dimensional least-squares identification (ID) or estimation problem that is based on the type of observations (i.e., sensors for data acquisition) available to us in experiments. We use a theoretically justifiable Galerkin methodology to reduce the infinite dimensional least-squares ID problems to a sequence of approximating finite dimensional ID problems which are computationally tractable. Solutions of the original problem can be then approximated by solutions of the finite dimensional problems.

In the next section we give an outline that conceptually describes this procedure in an abstract framework. This is followed by a description of the thermal-based methods we have employed. Finally we use the vibration testing beam example to give a brief comparison of our spline-based Galerkin approach to that in which one might use a more standard finite element construction of the approximate identification problems.

2 Methodology

To outline our basic methodology, we use a generic abstract parameter estimation problem similar to that given in [3]. For brevity, we consider here only second order in time systems (methods for first order in time systems, which includes the thermal NDE example, are detailed in [3]). We consider a parameter (q) dependent model in the weak or variational form

$$\begin{aligned} \ddot{w}(t) + A_2(q)\dot{w}(t) + A_1(q)w(t) &= f(t, q) \quad \text{in } V^* \\ w(0) &= w_0, \quad \dot{w}(0) = w_1 \end{aligned} \tag{2.1}$$

where the parameters q lie in an admissible set Q and the initial data satisfy $w_0 \in V$, $w_1 \in H$. Here V and H are Hilbert spaces which form a Gelfand triple $[W]$. That is, V is continuously and densely embedded in H , $V \hookrightarrow H$, and we identify H with its conjugate dual space H^* . The parameter-dependent operators $A_i(q)$ are continuous and linear from V to V^* , the conjugate dual of V . The duality pairing is denoted by $\langle \cdot, \cdot \rangle_{V^*, V}$ and thus for $\psi \in V$, $A_i(q)\psi \in V^*$ and we use the notation $(A_i(q)\psi)(\phi) = \langle A_i(q)\psi, \phi \rangle_{V^*, V}$ for all $\phi \in V$. With this notation, the

abstract system (2.1) can thus be written as

$$\begin{aligned} \langle \ddot{w}(t), \phi \rangle + \langle A_2(q)\dot{w}(t), \phi \rangle + \langle A_1(q)w(t), \phi \rangle &= \langle f(t, q), \phi \rangle \\ w(0) = w_0, \quad \dot{w}(0) = w_1 \end{aligned} \quad (2.2)$$

for all $\phi \in V$. Adopting somewhat commonly employed abbreviated notation, we let $\langle \cdot, \cdot \rangle$ denote $\langle \cdot, \cdot \rangle_{V^*, V}$ throughout the remainder of this discussion.

The admissible parameter set Q is assumed to lie in a metric space \tilde{Q} with metric d while the operators $A_i(q)$ are assumed to satisfy the following regularity hypotheses uniformly in $q \in Q$:

- (1) Symmetry: $\langle A_1(q)\phi, \psi \rangle = \overline{\langle A_1(q)\psi, \phi \rangle}$;
- (2) Boundedness: $|\langle A_i(q)\phi, \psi \rangle| \leq c_i |\phi|_V |\psi|_V$ with c_i independent of q ;
- (3) Coercivity: $\langle A_i(q)\phi, \psi \rangle \geq k_i |\phi|_V$ with k_i independent of q ;
- (4) Continuity with respect to parameters: $|\langle (A_i(q) - A_i(\tilde{q}))\phi, \psi \rangle| \leq \gamma d(q, \tilde{q}) |\phi|_V |\psi|_V$.

Under these assumptions, one can establish well-posedness of (2.1) (or equivalently, (2.2)) and then use it as the defining dynamical system in inverse or parameter estimation problems. (In fact, one can establish well-posedness under much weaker assumptions—see [10]).

One seeks to estimate the parameters q (e.g., coefficients in some DPS written abstractly as (2.1)) from dynamic observations of the system (2.1). This raises the important consideration as to what will be measured in the dynamic experiments from which we obtain our observations. In mechanical experiments, there are a number of popular measurement devices including accelerometers (yielding acceleration at a point on the structure), laser vibrometers (velocity), proximity probes (displacements), strain gauges (strain), and piezoceramic patches (accumulated strain) in smart structures. In thermal experiments one can use infrared sensors to provide measurements of temperature. For all such measurement devices, the resulting observations can be employed in a general least squares output formulation of the parameter estimation problem. In such cases, the problems are stated in terms of finding parameters which give the best fit of the parameter-dependent solutions of the partial differential equations to dynamic system response data collected with various excitations.

The general least squares parameter estimation problem can be formulated as follows. For a given discrete set of measured observations $z = \{z_i\}_{i=1}^{N_t}$ corresponding to model observations $z_{ob}(t_i)$ at times t_i as obtained in most practical cases, one considers the problem of minimizing over $q \in Q$ the least squares output functional

$$J(q, z) = \left| \tilde{C}_2 \left\{ \tilde{C}_1 \{w(t_i, \cdot; q)\} - \{z_i\} \right\} \right|^2, \quad (2.3)$$

where $\{w(t_i, \cdot; q)\}$ are the parameter dependent solutions of (2.1) evaluated at each time t_i , $i = 1, 2, \dots, N_t$ and $|\cdot|$ is an appropriately chosen Euclidean norm. Here the operators \tilde{C}_1 and \tilde{C}_2 are observation operators that depend on the type of observed or measured data that is available. The operator \tilde{C}_1 may have several forms depending on the type of sensors being used. For example, when the collected data z_i consists of time domain displacement, velocity,

or acceleration values at a point \bar{y} , the operator \tilde{C}_1 involves differentiation (either 0, 1, or 2 times, respectively) with respect to time followed by pointwise evaluation at t_i and \bar{y} .

While the most commonly encountered least squares problems involve time domain data, it is often advantageous to fit the data in a frequency domain setting. To treat these alternate possibilities, one may introduce a second observation operator \tilde{C}_2 . This operator \tilde{C}_2 may be the identity (corresponding to time domain identification procedures as already described) or may be related to the Fourier transform (corresponding to identification in the frequency domain). If the identification is carried out in the frequency domain and the operator \tilde{C}_2 is a Fourier transform related operator, then an appropriate cost functional is

$$\hat{J}(q, z) = \sum_{\ell=1}^{N_f} \left(\epsilon_1 |f_{k_\ell^w}(q) - f_{k_\ell^z}|^2 + \epsilon_2 \sum_{j=-n_\ell}^{N_\ell} \{|W(k_\ell^w + j; q)| - |Z(k_\ell^z + j)|\}^2 \right). \quad (2.4)$$

Here $W(k; q)$ and $Z(k)$ are the Fourier series coefficients of $\tilde{C}_1\{w(t_i, \bar{y}; q)\}$ and $\{z_i\}$ respectively, and $f_{k_\ell^w}$ and $f_{k_\ell^z}$ are the $(k_\ell^w)^{th}$ vibration frequency of the solution $W(k; q)$ and the $(k_\ell^z)^{th}$ frequency of the observation data $Z(k)$. Moreover, ϵ_1, ϵ_2 are weighting constants, and n_ℓ, N_ℓ are certain lower and upper limits associated with the width (or the support) of the ℓ^{th} spike. In formulating (2.4), one assumes that there are a finite and distinct number N_f of nontrivial “spikes”, i.e., vibration frequencies or “significant modes” among the $Z(k)$ and the number of nontrivial spikes of the solution $W(k; q)$ is the same as N_f . (Further details may be found in [10, 12].)

The minimization in these general abstract parameter estimation problems involves an infinite dimensional state space and possibly an infinite dimensional admissible parameter set (of functions). To obtain computationally tractable methods, one must consider some type of approximations in the context of the variational formulation (2.2). Let V^N be a sequence of finite dimensional subspaces of V , and Q^M be a sequence of finite dimensional sets approximating the parameter set Q . We denote by P^N the orthogonal projections of V onto V^N . Then a family of approximating estimation problems with finite dimensional state spaces and parameter sets can be formulated by seeking $q \in Q^M$ which minimizes

$$J^N(q, z) = \left| \tilde{C}_2 \{ \tilde{C}_1 \{ w^N(t_i, \cdot; q) \} - \{ z_i \} \} \right|^2, \quad (2.5)$$

where $w^N(t; q) \in V^N$ is the solution to the finite dimensional approximation of (2.2) given by

$$\begin{aligned} \langle \ddot{w}^N(t), \phi \rangle + \langle A_2(q) \dot{w}^N(t), \phi \rangle + \langle A_1(q) w^N(t), \phi \rangle &= \langle f(t, q), \phi \rangle \\ w^N(0) &= P^N w_0, \quad \dot{w}^N(0) = P^N \dot{w}_1, \end{aligned}$$

for $\phi \in V^N$.

Under reasonable (and verifiable) assumptions on Q, Q^M and V^N (e.g., compactness of Q, Q^M and convergence of Q^M to Q, V^N to V as $N, M \rightarrow \infty$ in an appropriate sense - see [3, 7, 10] for detailed statements), one can show that solutions \bar{q} and $\bar{q}^{N, M}$ to the minimization problems for (2.3) and (2.5), respectively, exist. Moreover, $\bar{q}^{N, M} \rightarrow \bar{q}$ in the metric of Q as $N, M \rightarrow \infty$.

3 Thermal NDE Methods

One application of the methodology outlined in the previous section is to the problem of detection and characterization of damages using thermal probes ([4, 5, 6]). To illustrate we consider a thin 2-D domain $G(q)$ as depicted in Figure 1. In this geometry the sides Γ and Γ_0 are assumed known while the back side $\partial G(q)$ is the damaged area that is not observable directly.

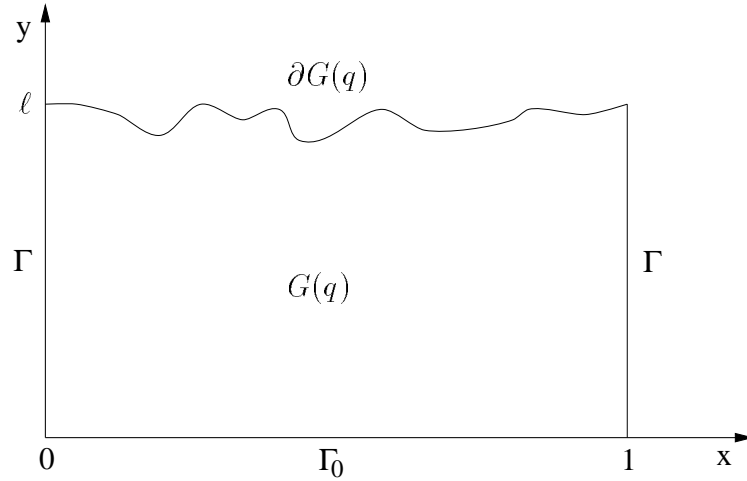


Figure 1. Thin 2-D sample with back surface damage

In experiments, the front surface Γ_0 is heated and a time record of the temperature on this surface is obtained using an infrared sensor. The sides Γ are assumed to be perfectly insulated while the damaged section is assumed to disrupt heat flow in a manner consistent with an insulated surface. Thus heat flow in the sample is described by the following model in strong form (α is the thermal diffusivity, κ is the thermal conductivity):

$$\begin{aligned} \frac{\partial u}{\partial t} - \alpha \Delta u &= 0 && \text{on } G(q) \\ u(0) &= u_0 && \text{on } G(q) \\ \frac{\partial u}{\partial n} &= 0 && \text{on } \Gamma \cup \partial G(q) \\ \kappa \frac{\partial u}{\partial n} &= f && \text{on } \Gamma_0. \end{aligned}$$

The associated inverse problems consist of estimating $\partial G(q)$ from observations of temperature u on Γ_0 . Also, the input f on Γ_0 is typically not directly measurable and must also be estimated from the surface temperatures. Both the surface $\partial G(q)$ and the input flux are assumed to be parameterized by some vector parameter q and we attempt to estimate a best value of q so that the model provides solutions with values on Γ_0 close to those observed in the experimental data.

A least squares fit of the time dependence of the temperature of the front surface of the sample can be used to attempt to determine the back surface geometry. This requires solving a partial differential equation (PDE) for shapes calculated from the parameters of the fit. Since no analytical solution is known for this case, a finite element technique can be used to solve the PDE. One approach to this problem would be to vary the finite element grid as a function of the parameters describing the shape of the objects. This approach however is computationally difficult and may lead to discontinuities in the derivatives of the solutions with respect to the parameters (an unpleasant situation for most optimization codes). A second approach involves using the method of mappings which is computationally much simpler.

The method of mappings transforms the problem of solving a relatively simple PDE on a complex geometry to a coordinate system where the complexity is shifted to the PDE and the geometry is relatively simple. Details of the application of this technique to this type of problem are given in [6]. In the example described here, the shape of the sample was mapped into a coordinate system where the shape of the sample was rectangular.

The sample here is taken to be a thin plate with a rectangular geometry, with the exception of a portion of the back surface. The variation in the back surface shape is assumed the same for the thickness of the plate; therefore the heat flow is two dimensional. The shape of the back surface is assumed to be given by $r(x)$ with a constraint on the shape requiring that $r(0)$ and $r(1)$ are both equal to ℓ . The case of $r(x)$ equal to ℓ for all x corresponds to a rectangular geometry for the plate (i.e., no damage). We assume that the initial temperature u_0 of the sample is known.

The variational form of this problem can be written as

$$\int_{G(q)} \left(\frac{\partial u}{\partial t} \phi + \alpha \nabla u(t) \cdot \nabla \phi \right) dV = \int_{\Gamma_0} \frac{\alpha}{\kappa} f \tau \phi ds .$$

Here $G(q)$ is the two dimensional plate volume, Γ_0 is the boundary corresponding to $y = 0$, τ denotes the trace operator on Γ_0 and ϕ is any member of the class of test functions used in formulating the variational equation (see [6] for details). This problem can be transformed to a coordinate system where the shape of the plate was rectangular using the transformation $x = x_2$, and $y = y_2 r(x_2) / \ell$. For this coordinate system the variational form is given by the expression (again see [6])

$$\begin{aligned} \int_{V_2} \alpha \left[\frac{\partial \tilde{u}}{\partial x_2} \frac{\partial \tilde{\phi}}{\partial x_2} - \frac{r' y_2}{r} \left(\frac{\partial \tilde{u}}{\partial x_2} \frac{\partial \tilde{\phi}}{\partial y_2} + \frac{\partial \tilde{u}}{\partial y_2} \frac{\partial \tilde{\phi}}{\partial x_2} \right) + \frac{(r')^2 y_2^2 + \ell^2}{r^2} \frac{\partial \tilde{u}}{\partial y_2} \frac{\partial \tilde{\phi}}{\partial y_2} \right] dV_2 \\ + \int_{V_2} \left[\frac{\partial \tilde{u}}{\partial t} - \alpha \frac{r'}{r} \frac{\partial \tilde{u}}{\partial x_2} + \alpha \frac{(r')^2}{r^2} y_2 \frac{\partial \tilde{u}}{\partial y_2} \right] \tilde{\phi} dV_2 = \int_{\Gamma_0} \frac{\alpha}{\kappa} f \tau \tilde{\phi} \frac{\ell}{r} ds \end{aligned}$$

where \tilde{u} and $\tilde{\phi}$ refer to the temperature and test functions in the transformed coordinate system, respectively, and V_2 is the rectangular region $0 \leq x_2 \leq 1$, $0 \leq y_2 \leq \ell$. As can be seen by a comparison of equations, the transformation of coordinate system transfers the complexity of the problem to the PDE. However, computationally it is easier to solve the transformed equation than to solve a problem involving variation of the grid to account for variation in shape of the domain.

To carry out the least-squares optimization in this problem, the curve $r(x)$ and the input f were parameterized by a finite dimensional vector parameter (again call it q). In this case, linear interpolation was used and best fit piecewise linear \bar{r} , \bar{f} were obtained. A first order in time version of the methodology outlined in Section 2 was used to provide theory and computational methods. Bilinear splines were used for the Galerkin approximations of the thermal dynamics. Complete details including the successful identification of damage from experimental data are given in [6].

4 Numerical Methods for Beam Damage Detection

To illustrate the damage detection methodology of Section 2 in the context of dynamic structural models with variable coefficients, we consider here a damaged cantilever beam. For this discussion, it is assumed that a single pair of piezoceramic patches with edges at y_1, y_2 are mounted to the surface of a beam of length ℓ as depicted in Figure 2. The thickness of the beam and patches are denoted by h and h_{pe} , respectively, while both beam and patches are assumed to have width b . Furthermore, it is assumed that the beam is damaged by a circular hole of radius r and center y_c .

In this section, numerical techniques satisfying the hypotheses of Section 2 will be discussed to illustrate the issues which must be considered when implementing PDE-based damage detection methods. A Galerkin-based spline approximate will be compared with a standard Hermite finite element method to emphasize the issues. While the development is specific to the beam example, similar issues must be addressed when developing numerical methods for implementing PDE-based damage detection techniques for complex structures.

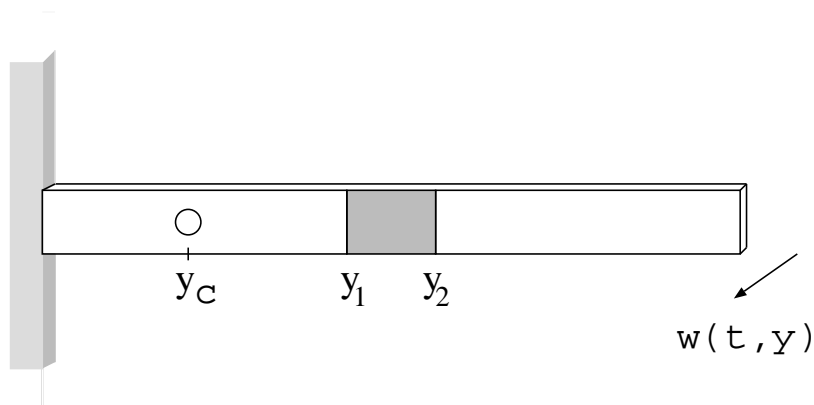


Figure 2. Cantilever beam with surface-mounted piezoceramic patches and a hole of radius r centered at y_c .

4.1 Strong Form of Model

As detailed in [2, 10], moment and force balancing (Newton's laws) can be used to obtain a strong form of the modeling equations

$$\tilde{\rho}(y)\dot{w}(t, y) + \gamma\dot{w}(t, y) + [\widetilde{c}_D(y)\dot{w}''(t, y) + \widetilde{E}I(y)w''(t, y)]'' = f(t, y) \quad (4.1)$$

with the essential boundary conditions

$$w(t, 0) = w'(t, 0) = 0 \quad (4.2)$$

at the fixed end and the natural boundary conditions

$$(\widetilde{c}_D(y)\dot{w}''(t, y) + \widetilde{E}I(y)w''(t, y))|_{y=\ell} = 0$$

$$(\widetilde{c}_D(y)\dot{w}''(t, y) + \widetilde{E}I(y)w''(t, y))'|_{y=\ell} = 0$$

at the free end. In this Euler-Bernoulli model, w denotes the transverse beam displacement, f denotes distributed surface forces on the beam and \dot{w}, w' denote temporal and spatial derivatives, respectively. Due to the presence of the patches and damage, the structural density, stiffness and Kelvin-Voigt parameters $\tilde{\rho}(y), \widetilde{E}I(y)$ and $\widetilde{c}_D I(y)$ are spatially varying and have the forms

$$\tilde{\rho}(y) = \rho h b + 2\rho_{pe} h_{pe} b \chi_{pe}(y) - \rho S_A(y) \chi_d(y)$$

$$\widetilde{E}I(y) = E \frac{1}{12} h^3 b + E_{pe} \frac{2}{3} a_3 b \chi_{pe}(y) - E S_I(y) \chi_d(y)$$

$$\widetilde{c}_D I(y) = c_D \frac{1}{12} h^3 b + c_{Dpe} \frac{2}{3} a_3 b \chi_{pe}(y) - c_D S_I(y) \chi_d(y) .$$

The patch and damage components are localized to their respective regions by the characteristic functions

$$\chi_{pe}(y) = \begin{cases} 1 & y \in [y_1, y_2] \\ 0 & \text{otherwise} \end{cases}, \quad \chi_d(y) = \begin{cases} 1 & y \in [y_c - r, y_c + r] \\ 0 & \text{otherwise} \end{cases} .$$

Furthermore, $a_3 \equiv (h/2 + h_{pe})^3 - (h/2)^3$ while E, E_{pe} , and c_D, c_{Dpe} are the Young's moduli and Kelvin-Voigt damping coefficients of the beam and the piezoceramic patches, respectively. The general shape functions S_A and S_I indicate the area and moment of inertia of the missing region.

For the specific case of a circular hole with center y_c and radius r , these shape functions can be represented as $S_A(y) = hS(y)$, $S_I(y) = \frac{1}{12}h^3bS(y)$ where

$$S(y) = 2\sqrt{r^2 - (y - y_c)^2} .$$

The reader is referred to [2, 10] for discussion of more general shape functions. Furthermore, if the force to the beam is provided solely through input of a voltage $u(t)$ to the patches, f is given by

$$\mathcal{K}^B \chi_{pe}''(y) u(t)$$

where $\mathcal{K}^B = (h + h_{pe})bE_{pe}d_{31}$ (see [8]).

Due to the discontinuities in the physical parameters and control inputs which are due to the patches, classical solutions ($w(t, y) \in H^4(0, \ell)$) cannot be obtained to (4.6). To alleviate such difficulties and to reduce smoothness requirements on basis functions, it is advantageous to consider a weak form of the modeling equations derived via Hamilton's principle.

4.2 Weak Form Via Hamilton's Principle

We illustrate first the conservative case (no damping or force). With T, U denoting the kinetic and potential energy, respectively, Hamilton's principle states that dynamics of the beam yield a stationary value of the action integral

$$A[w] = \int_{t_0}^{t_1} (T - U) dt ,$$

for arbitrary t_0, t_1 when compared with admissible variations Φ in the motion [17]. This requirement can be expressed as

$$\frac{d}{d\varepsilon} A[w + \varepsilon\Phi] \Big|_{\varepsilon=0} = 0 . \quad (4.3)$$

For the beam under consideration, the kinetic and potential energies are given by

$$T(t) = \frac{1}{2} \int_0^\ell \tilde{\rho}(y) (\dot{w}(t, y))^2 dy$$

$$U(t) = \frac{1}{2} \int_0^\ell \widetilde{EI}(y) (w''(t, y))^2 dy .$$

The admissible variations are assumed to be of the form $\Phi = \eta(t)\phi(x)$ where $\eta(t_1) = \eta(t_2) = 0$ and $\phi \in V = H_L^2(0, \ell) \equiv \{v \in H^2(0, \ell) : v(0) = v'(\ell) = 0\}$. Expansion of the functional in (4.8) and integration by parts in time then yields the weak formulation

$$\int_0^\ell (\tilde{\rho}(y) \ddot{w}\phi + \widetilde{EI}(y) w''\phi'') dy = 0$$

which must hold for all $\phi \in H_L^2(0, \ell)$.

Inclusion of damping contributions and external forces and/or moments can be accomplished via an extended Hamilton's principle. For the damped beam subject to forces generated through piezoceramic patch inputs, this yields the weak form

$$\int_0^\ell [\tilde{\rho}(y) \ddot{w}\phi + \gamma \dot{w}\phi + \widetilde{EI}(y) w''\phi'' + \widetilde{c}_D(y) \dot{w}'\phi'] dy = \left(\int_{y_1}^{y_2} \mathcal{K}^B \phi'' dy \right) u(t) \quad (4.4)$$

for all $\phi \in V$. It should be noted that smoothness requirements on the solutions w are reduced and this makes the weak form appropriate for consideration of the beam (as well as more general structures) with embedded or surface-mounted actuators. For cases in which parameters and control inputs are sufficiently smooth to yield $w \in H^4(0, \ell)$, integration by parts can be used to demonstrate the equivalence of the strong form (4.6) and weak form (4.9).

To place the model in the framework of Section 2, we take $H = L^2(0, \ell)$ and $V = H_L^2(0, \ell)$ as defined above. With the inner products

$$\langle \psi, \phi \rangle_H = \int_0^\ell \tilde{\rho} \psi \phi dy$$

$$\langle \psi, \phi \rangle_V = \int_0^\ell \widetilde{EI} \psi'' \phi'' dy ,$$

the embedding $V \hookrightarrow H$ is dense and continuous. The duality product $\langle \cdot, \cdot \rangle_{V^*, V}$ is then the extension by continuity of the inner product $\langle \cdot, \cdot \rangle_H$ from $V \times H$ to $V^* \times H$. The operators $A_i(q) : V \rightarrow V^*$, $i = 1, 2$, are defined by

$$\begin{aligned} (A_1(q)\psi)(\phi) &= \int_0^\ell \widetilde{EI} \phi'' \psi'' dy \\ (A_2(q)\psi)(\phi) &= \int_0^\ell \widetilde{c_D I} \phi'' \psi'' dy . \end{aligned}$$

With the input operator $B \in \mathcal{L}(U, V^*)$, where U is the input space, given by

$$\langle Bu(t), \phi \rangle_{V^*, V} = \int_{y_1}^{y_2} \mathcal{K}^B \phi'' dy \cdot u(t) ,$$

the system (4.9) is equivalent to the operator equation (2.1) in V^* or the weak form (2.2) with $f(t) = Bu(t)$.

The operators A_1, A_2 defined in this manner satisfy the symmetry, boundedness, coercivity and parameter continuity conditions described in Section 2. When combined with the approximation techniques discussed next, the results of Section 2 yield a theoretically rigorous and computationally tractable method for estimating the unknown structural parameters which include damage criteria.

4.3 Galerkin Spline Approximation

One technique for approximating the solutions to (4.9) is through cubic B-spline expansions in a Galerkin setting. The basis in this case is constructed from canonical cubic B-splines $\{\tilde{\phi}_i\}$ of the form illustrated in Figure 3 (see [16, pages 78-80] for details regarding the definition of these splines). Because the canonical splines satisfy the relations $\tilde{\phi}_i(x_i) = 4$, $\tilde{\phi}_i(x_{i-1}) = \tilde{\phi}_i(x_{i+1}) = 1$ and $\tilde{\phi}'_i(x_i) = 0$, $\tilde{\phi}'_i(x_{i-1}) = 1$, $\tilde{\phi}'_i(x_{i+1}) = -1$ when mapped to the interval $[x_{i-2}, x_{i+2}]$, the choice

$$\begin{aligned} \phi_1(y) &= \tilde{\phi}_0(y) - 2\tilde{\phi}_{-1}(y) - 2\tilde{\phi}_1(y) \\ \phi_i(y) &= \tilde{\phi}_i(y) \quad , \quad i = 2, \dots, N+1 \end{aligned}$$

yields a basis $\{\phi_i\}_{i=1}^{N+1}$ which satisfies the essential boundary conditions (4.7). One then defines the approximating space $V^N = \text{span}\{\phi_i\} \subset V$ and constructs approximate solutions through the expansion

$$w^N(t, y) = \sum_{j=1}^{N+1} w_j^N(t) \phi_j(y) . \tag{4.5}$$

This approximation technique satisfies the necessary convergence criteria alluded to in Section 2 and is computationally efficient and accurate.

It should be noted that *through construction*, the splines have continuous first and second derivatives. By incorporating all smoothness constraints in the basis, the problem is reduced from that of finding a solution which satisfies mixed interpolatory and smoothness constraints to one which is purely interpolatory. This will be in contrast to finite element techniques in which degrees of freedom arise from mixed constraints.

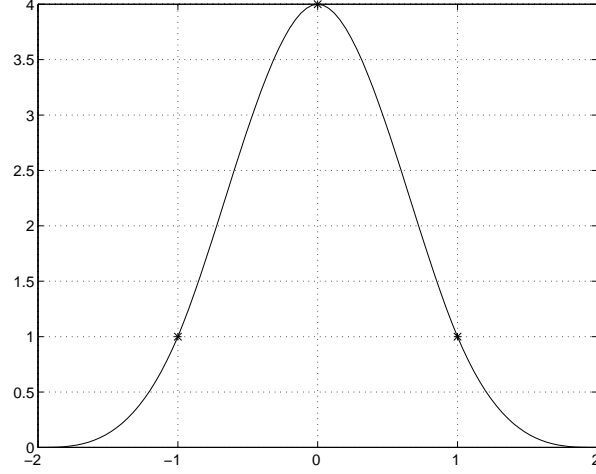


Figure 3. Canonical cubic spline $\tilde{\phi}_i(x)$ on the reference interval $[-2, 2]$.

Orthogonalization of the residual with respect to basis functions then yields the approximating ODE system

$$M^N \ddot{\mathcal{W}}^N(t) + C^N \dot{\mathcal{W}}^N(t) + K^N \mathcal{W}^N(t) = F^N u(t)$$

where the mass, stiffness and forcing components are defined by

$$M^N = \begin{bmatrix} \int_0^\ell \tilde{\rho} \phi_1 \phi_1 dy & \cdots & \int_0^\ell \tilde{\rho} \phi_{N+1} \phi_1 dy \\ \vdots & & \vdots \\ \int_0^\ell \tilde{\rho} \phi_1 \phi_{N+1} dy & \cdots & \int_0^\ell \tilde{\rho} \phi_{N+1} \phi_{N+1} dy \end{bmatrix},$$

$$K^N = \begin{bmatrix} \int_0^\ell \widetilde{EI} \phi_1'' \phi_1'' dy & \cdots & \int_0^\ell \widetilde{EI} \phi_1'' \phi_{N+1}'' dy \\ \vdots & & \vdots \\ \int_0^\ell \widetilde{EI} \phi_{N+1}'' \phi_1'' dy & \cdots & \int_0^\ell \widetilde{EI} \phi_{N+1}'' \phi_{N+1}'' dy \end{bmatrix}$$

$$F^N = \begin{bmatrix} \int_{y_1}^{y_2} \mathcal{K}^B \phi_1'' dy \\ \vdots \\ \int_{y_1}^{y_2} \mathcal{K}^B \phi_{N+1}'' dy \end{bmatrix}$$

and $\mathcal{W}^N(t) = [w_1^N(t), \dots, w_{N+1}^N(t)]^T$ contains the generalized Fourier coefficients.

The approximate solution at time t is determined by solving the ODE system to that point and constructing the solution through the expansion (4.10). We reiterate that the coefficients $\tilde{\rho}(y)$, $\widetilde{EI}(y)$, $\widetilde{c_D I}(y)$ are spatially varying due to the nonhomogeneities from the patches and damage.

4.4 Finite Element Analysis

A second approximation method which is widely used in structural applications is the finite element method. While this latter method shares a common mathematical background with

the previously described spline-based Galerkin technique, the manner of application is sufficiently different to warrant discussion. We present the technique from two perspectives. The first is formal and is intended to illustrate the construction of the resulting matrix system and highlight issues which must be addressed when employing the finite element method in damage detection applications. Once the method has been illustrated in this manner, we place it in a rigorous mathematical framework through a brief discussion of the Ciarlet triple and appropriate approximation spaces.

The basic strategy in the finite element method is to consider the structure as an assemblage of individual elements as depicted in Figure 4. Associated with a typical element are nodal points at which we will define parameters which ultimately define the beam displacement. In this case, each element has two nodal points which are located at the element ends. Possible motions at the nodes are described as *local* degrees of freedom (local DOF). For the beam elements, displacements and rotations (slopes) are considered at each end of the element. This yields a total of 4 local DOF for the element. The displacements result from nodal forces whereas nodal moments yield the rotations. Note that by specifying both displacements and slopes, we will obtain a *Hermite* finite element as compared with *Lagrangian* elements in which only displacements are specified.

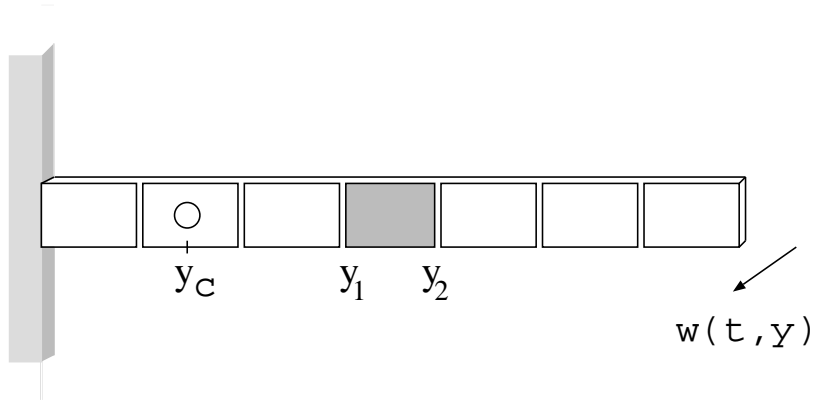


Figure 4. Finite element discretization of the cantilever beam.

To uniquely determine the displacements and slopes at the element edges (4 local DOF), polynomials of at least degree 3 are required. These polynomials are typically defined on a local interval \mathcal{K} with local nodal values matched to obtain global displacements. To illustrate, we consider an element of length L located between ℓ_1 and ℓ_2 ; hence $\mathcal{K} = [0, L]$. On this interval, the local (element) deflections are taken of the form

$$w_L^e(t, y) = a_0(t) + a_1(t)y + a_2(t)y^2 + a_3(t)y^3. \quad (4.6)$$

With the notation $\{A(t)\}^T = [a_0(t), a_1(t), a_2(t), a_3(t)]$ and $\{z(y)\} = [1, y, y^2, y^3]^T$, the approx-

imate solution and squared strain can be expressed as

$$\begin{aligned} w_L^e(t, y) &= \{A(t)\}^T \{z(y)\} \\ \left(\frac{\partial^2 w_L^e}{\partial y^2}(t, y)\right)^2 &= \{A(t)\}^T \{z''(y)\} \{z''(y)\}^T \{A(t)\} \\ &= \{A(t)\}^T [D(y)] \{A(t)\}, \end{aligned}$$

where $[D(y)] \equiv \{z''(y)\} \{z''(y)\}^T$ is a 4×4 matrix. Moreover if we define

$$\begin{aligned} w_1(t) &= w_L^e(t, 0) \quad , \quad w_2(t) = w_L^e(t, L) \\ \theta_1(t) &= \frac{\partial w_L^e}{\partial y}(t, 0) \quad , \quad \theta_2(t) = \frac{\partial w_L^e}{\partial y}(t, L) \end{aligned}$$

then enforcement of (4.11) yields

$$\{w(t)\}_i = \begin{bmatrix} w_1(t) \\ \theta_1(t) \\ w_2(t) \\ \theta_2(t) \end{bmatrix} = [B] \{A(t)\} \quad , \quad [B] = \begin{bmatrix} 1 & 0 & 0 & 0 \\ 0 & 1 & 0 & 0 \\ 1 & L & L^2 & L^3 \\ 0 & 1 & 2L & 3L^2 \end{bmatrix}$$

where $\{w(t)\}_i$ contains the nodal displacements and slopes. Equivalently, with C defined as B^{-1} , the original coefficients can be expressed as $\{A(t)\} = [C] \{w(t)\}_i$. This then implies that w_L^e can be represented as

$$w_L^e(t, y) = \{z(y)\}^T [C] \{w(t)\}_i. \quad (4.7)$$

To determine the motion, Hamilton's principle is again invoked. Demonstrating first with the conservative case, the potential and kinetic energies for the element are expressed as

$$\begin{aligned} U &= \frac{1}{2} \int_0^L \widetilde{EI}(y) \left(\frac{\partial^2 w_L^e}{\partial y^2}(t, y)\right)^2 dy \\ &= \{w(t)\}_i^T [C]^T \cdot \frac{1}{2} \int_0^L \widetilde{EI}(y) [D(y)] dy \cdot [C] \{w(t)\}_i \end{aligned}$$

and

$$T = \{\dot{w}(t)\}_i^T [C]^T \cdot \frac{1}{2} \int_0^L \tilde{\rho}(y) [F(y)] dy \cdot [C] \{\dot{w}(t)\}_i$$

where $[F(y)] \equiv \{z(y)\} \{z(y)\}^T$. Hamilton's principle then yields

$$[M^e] \{\ddot{w}(t)\}_i + [K^e] \{w(t)\}_i = 0 \quad (4.8)$$

where

$$[M^e] = [C]^T \cdot \int_0^L \tilde{\rho}(y) [F(y)] dy \cdot [C]$$

$$[K^e] = [C]^T \cdot \int_0^L \widetilde{EI}(y) [D(y)] dy \cdot [C]$$

denote the *local* mass and stiffness matrices.

The vector equation (4.13) describes the dynamics of the unforced and undamped local element on $[\ell_1, \ell_2]$. To obtain global equations, the local dynamics are matched through enforcement of compatibility conditions regarding displacements and rotations (slopes). Specifically, displacement and rotations at the element nodes are required to match those of neighboring elements. This is analogous to noting that moments and forces at the adjacent nodes are balanced.

To illustrate, we consider a simplified case in which a *homogeneous* beam (hence constant parameters) is discretized into two identical elements. The local stiffness matrix in this case has the structure

$$[K^e] = \frac{EI}{L^3} \begin{bmatrix} 12 & 6L & -12 & 6L \\ 6L & 4L^2 & -6L & 2L^2 \\ -12 & -6L & 12 & -6L \\ 6L & 2L^2 & -6L & 4L^2 \end{bmatrix}.$$

Enforcement of displacement and rotational components yields the global stiffness matrix

$$[K] = \frac{EI}{L^3} \begin{bmatrix} 12 & 6L & -12 & 6L & 0 & 0 \\ 6L & 4L^2 & -6L & 2L^2 & 0 & 0 \\ -12 & -6L & 24 & 0 & -12 & 6L \\ 6L & 2L^2 & 0 & 8L^2 & -6L & 2L^2 \\ 0 & 0 & -12 & -6L & 12 & -6L \\ 0 & 0 & 6L & 2L^2 & -6L & 4L^2 \end{bmatrix}.$$

Note that in constructing the global system, the number of *global* DOF is the total number of local DOF minus the number of enforced compatibility conditions.

The nonconservative damping and external effects are incorporated via an extended Hamilton's principle as mentioned in Section 4.2. We emphasize that when considering the beam having surface-mounted piezoceramic patches and missing material at y_c , the density, stiffness and damping parameters are *not* constant and quadrature rules must be employed when constructing the local mass, stiffness and damping matrices. Due to the piecewise nature of the parameters, the elements must be aligned with patch edges to preserve the accuracy of the method and care must be exercised when enforcing compatibility constraints. In summary, routines which admit spatial variability (including piecewise discontinuities) *must* be employed to obtain success when employing finite elements in damage detection schemes using piezoceramic actuators and sensors.

4.4.1 Mathematical Formulation of the Finite Element Method

To place the method in the Sobolev framework outlined in Section 2, it is advantageous to consider a slightly more abstract definition of a finite element and using this, construct approximating subspaces. Following the definition of Ciarlet [14], a finite element is defined as the triple $(\mathcal{K}, \mathcal{P}, \mathcal{N})$ where \mathcal{K} denotes a local geometrical region, \mathcal{P} is a finite dimensional space of functions on \mathcal{K} , and \mathcal{N} is the degrees of freedom [13, 14]. For this discussion, $\mathcal{K} = [0, L] \subset [0, \ell]$ is an interval, $\mathcal{P} = P_3$ denotes the set of cubic polynomials and $\mathcal{N} = \{N_1, N_2, N_3, N_4\}$ where $N_1(v) = v(0)$, $N_2(v) = v'(0)$, $N_3(v) = v(L)$, $N_4(v) = v'(L)$ for all $v \in \mathcal{P}$. Note that \mathcal{N} forms a basis for the dual space \mathcal{P}^* .

For the finite element $(\mathcal{K}, \mathcal{P}, \mathcal{N})$, we let $\{\psi_1, \psi_2, \psi_3, \psi_4\}$ denote a basis for $\mathcal{P} = P_3$ on the interval \mathcal{K} . In terms of the previous discussion, this basis, termed the *nodal basis*, is given by $\{z\}^T[C]$ for $\mathcal{K} = [0, L]$ (see (4.12)). For $L = 1$, the four basis functions are plotted in Figure 5. Note that $N_i(\psi_j) = \delta_{ij}$ for $i, j = 1, \dots, 4$.

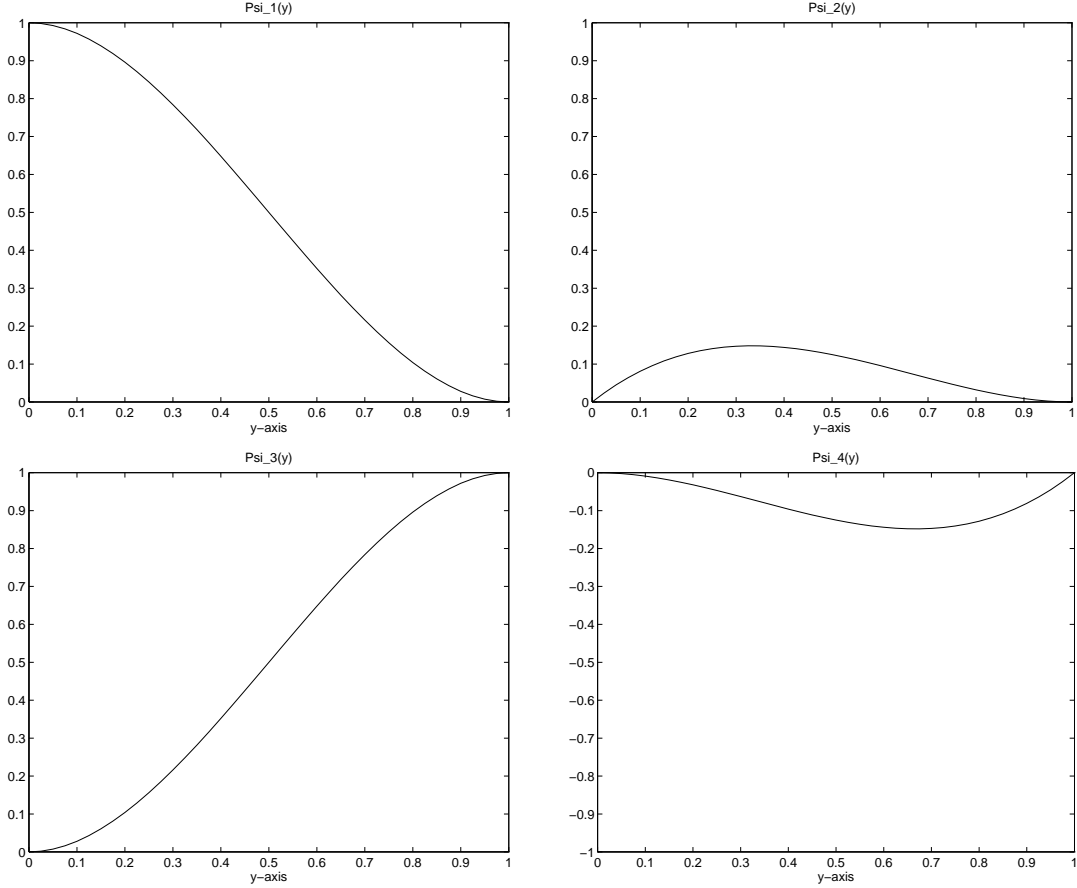


Figure 5. Local Hermite basis functions $\psi_1(y), \psi_2(y), \psi_3(y), \psi_4(y)$ defined on the interval $[0, L] = [0, 1]$.

The *local interpolant* is then defined by the expansion

$$\mathcal{I}_{\mathcal{K}}v \equiv \sum_{j=1}^4 N_j(v)\psi_j$$

(see [13, 14] for the general formulation of the local interpolant). Note that in the notation of the previous discussion, the nodal values are given by $\{w_i\} = [w_1, \theta_1, w_2, \theta_2]^T$ and the local interpolant is represented by $w_L^\epsilon = \{z\}^T[C]\{w\}_i$ (again see (4.12)).

With local interpolants thus defined, it is necessary to define a *global interpolant* over the full domain. To this end, let \mathcal{T} denote a subdivision of $[0, \ell]$ into a set of subintervals K_j with $[0, \ell] = \bigcup \overline{K_j}$. The global interpolant $\mathcal{I}_{\mathcal{T}}$ is then defined as

$$\mathcal{I}_{\mathcal{T}}g|_{K_j} = \mathcal{I}_{K_j}g$$

for $g \in C^1[0, \ell]$ and $K_j \in \mathcal{T}$. By matching nodal values (hence displacements and slopes) between elements, $\mathcal{I}_{\mathcal{T}}g \in C^1$ for all $g \in C^1[0, \ell]$ and the space $V^N = V_h \subset C^1[0, \ell]$ defined by

$$V_h = \{g : g|_{K_j} \in P_3(K_j) \text{ for all } K_j \in \mathcal{T}, \text{ and } g, g' \text{ continuous at the nodes}\}$$

is termed a C^1 finite element space (the notation V_h is common in the finite elements literature and we retain it here to denote the approximating finite dimensional space). It is this space V_h which is considered in the approximation framework of Section 2. The reader is reminded that the regularity of the finite element space depends on the dimension and while the Hermite elements described here yield C^1 interpolants on the interval, they will yield only C^0 interpolants when triangulating in \mathbb{R}^2 (see [13] and [15, pages 80,81]).

The finite element approach differs from the previously discussed cubic spline Galerkin method in the local-to-global nature of the approximation. Through an affine mapping of basis functions on a reference element $[0, L]$ to $[\ell_1, \ell_2]$, local interpolants are constructed. Like the cubic spline approximates, these local interpolants satisfy a smoothness criteria dictated by the choice of basis. Global interpolants are then obtained through enforcement of nodal compatibility criteria. This yields a C^1 method satisfying mixed smoothness and interpolatory criteria. The requirement of matching nodal displacements and slopes is unnecessary with the cubic spline basis since all smoothness properties are directly constructed in the basis. This yields a C^2 approximate solution which satisfies purely interpolatory constraints.

5 Conclusion

This brief review has centered on a nondestructive evaluation (NDE) technology based upon PDE models of the physical system of interest. By formulating the method in an abstract operator setting, one obtains well-posedness and a convergence theory which is sufficiently general to include NDE applications ranging from thermal imaging to vibration analysis with smart material sensors and actuators.

A key component in the implementation of the method is the choice of approximation scheme when discretizing the PDE model to obtain a matrix system. Due to the *local* nature of actuator inputs and damage, approximation methods employing locally defined basis functions appear to yield superior sensitivity when solving the inverse problem to estimate physical parameters. As demonstrated in investigations referenced in [2, 10], methods based upon globally defined modal bases and frequency shifts lack the sensitivity to adequately locate and characterize damage in general applications (the sensitivity often lies below the threshold of measurement error). On the other hand, cubic spline based Galerkin methods have been successfully employed to characterize damage representing less than 0.1% of the undamaged structural state. Due to the issue of sensitivity with respect to local structural variations, it is also hypothesized that Galerkin expansions employing globally defined Legendre or Chebyshev bases will prove less successful in NDE applications than those employing spline or finite element bases.

The success of either the spline-based Galerkin methods or finite element approaches is contingent upon the construction of approximate solutions which admit variable physical parameters (including piecewise discontinuities). To retain accuracy with either approach, gridpoints must be aligned with the discontinuities (e.g., patch edges). This can be a limitation

for codes employing automatic mesh-independent error analysis. The same issue must be faced if parameter discontinuities occur due to the nature of the damage. The determination of an appropriate mesh is more difficult in this latter case, however, since the region of discontinuity is unknown and is to be determined through parameter estimation.

The models and numerical methods must also be flexible with regards to boundary conditions. While this issue may at first appear unrelated to the ultimate goal of damage detection, it is in fact crucial for attaining sufficient accuracy to detect material nonhomogeneities. Both numerical investigations [9] and experiments [1] have illustrated the necessity of modeling inexact boundary conditions for structures with boundary energy loss as compared with the option of compensating through modification of structural parameters (e.g., increased ρ and decreased E will decrease *some* frequencies in a manner similar to loosened boundary clamps). As illustrated in [1, 9], however, this latter technique does *not* provide accurate model fits over a significant frequency range nor does it lead to consistency among estimated parameters. From an NDE perspective, it is flawed since the modification of physical parameters to account for boundary inaccuracies will tend to reduce the accuracy for determining variations due to damage. Hence numerical methods (either spline or finite element) must be sufficiently flexible to approximate boundary variations which are incorporated in the PDE model.

Acknowledgements This research was supported in part by the Air Force Office of Scientific Research under grants AFOSR-F49620-93-1-0198 and AFOSR-F49620-95-1-0236, by NASA under grant NAG-1-1600 and by the U.S. Department of Education through a GAANN Fellowship to Y.Z.

References

- [1] H.T. Banks, D.E. Brown, R.J. Silcox, R.C. Smith and Y. Wang, Modeling and estimation of boundary parameters for imperfectly clamped structures, to appear.
- [2] H.T. Banks, D.J. Inman, D.J. Leo and Y. Wang, An experimentally validated damage detection theory in smart structures, CRSC Technical Report CRSC-TR95-7, January, 1995; *Journal of Sound and Vibration*, to appear.
- [3] H.T. Banks and K. Ito, A unified framework for approximation in inverse problems for distributed parameter systems, in *Control: Theory and Advanced Technology*, 4(1), 1988, pp. 73-90.
- [4] H.T. Banks and F. Kojima, Approximation techniques for domain identification in two dimensional parabolic systems under boundary observations, Proc. 26th IEEE Conf. on Dec. and Control, December, 1987, Los Angeles, 1411-1416.
- [5] H.T. Banks and F. Kojima, Boundary shape identification problems in two dimensional domains related to thermal testing of materials, *Quart. Applied Math.*, 47, 1989, pp. 273-293.
- [6] H.T. Banks, F. Kojima and W.P. Winfree, Boundary estimation problems arising in thermal tomography, *Inverse Problems*, 6, 1990, pp. 897-921.

- [7] H.T. Banks and K. Kunisch, *Estimation Techniques for Distributed Parameter Systems*, Birkhäuser Boston, 1989, 320 pp.
- [8] H.T. Banks, R.C. Smith and Y. Wang, The modeling of piezoceramic patch interactions with shells, plates and beams, *Quart. Applied Math.*, 53, 1995, pp. 353-387.
- [9] H.T. Banks, R.C. Smith and Y. Wang, Parameter estimation for an imperfectly clamped plate – numerical examples, Proceedings of the 1995 Design Engineering Technical Conferences, Volume 3, Part C, Boston, MA, September 17-20, 1995, 963-972.
- [10] H.T. Banks, R.C. Smith and Y. Wang, *Smart Material Structures: Modeling, Estimation and Control*, CRSC Lecture Notes CRSC-LN96-1, March, 1996; Masson/J. Wiley, to appear.
- [11] H.T. Banks and Y. Wang, Damage detection and characterization in smart material structures, CRSC Technical Report CRSC-TR93-17, November 1993; in *Control and Estimation of Distributed Parameter Systems; Nonlinear Phenomena*, Birkhäuser ISNM, 118, 1994, pp. 21-43.
- [12] H.T. Banks, Y. Wang and D.J. Inman, Bending and shear damping in beams: frequency domain estimation techniques, *ASME J. Vibration and Acoustics*, 116, 1994, pp. 188-197.
- [13] S.C. Brenner and L.R. Scott, *The Mathematical Theory of Finite Element Methods*, Springer-Verlag, New York, 1994.
- [14] P.G. Ciarlet, *The Finite Element Method for Elliptic Problems*, North Holland, New York, 1978.
- [15] C. Johnson, *Numerical Solution of Partial Differential Equations by the Finite Element Method*, Cambridge University Press, New York, 1987.
- [16] P.M. Prenter, *Splines and Variational Methods*, Wiley, New York, 1975.
- [17] R. Weinstock, *Calculus of Variations with Applications to Physics and Engineering*, Dover, New York, 1974.
- [18] J. Wloka, *Partial Differential Equations*, Cambridge University Press, Cambridge, 1987.